electronic reprint

Journal of
Applied Crystallography
ISSN 0021-8898
Editor: **Gernot Kostorz**

Scattering from laterally heterogeneous vesicles. I. Model-independent analysis

Jeremy Pencer, Vinicius N. P. Anghel, Norbert Kučerka and John Katsaras

Journal of
Applied Crystallography
ISSN 0021-8898

Received 28 June 2006
Accepted 31 August 2006

Scattering from laterally heterogeneous vesicles. I. Model-independent analysis

Jeremy Pencer,[a]* Vinicius N. P. Anghel,[b] Norbert Kučerka[a] and John Katsaras[a,c]

[a]National Research Council, Canadian Neutron Beam Centre, Chalk River Laboratories, Building 459, Station 18, Chalk River, ON, K0J 1J0, Canada, [b]Atomic Energy of Canada Ltd, Chalk River Laboratories, Chalk River, ON, K0J 1J0, Canada, and [c]Department of Physics, Guelph Waterloo Physics Institute and Biophysics Interdepartmental Group, University of Guelph, Guelph, ON, N1G 2W1, Canada. Correspondence e-mail: jeremy.pencer@nrc.gc.ca

This is the first of a series of papers considering the scattering from laterally heterogeneous vesicles. Here, it is shown that contrast variation studies on unilamellar vesicles can be analyzed in a model-independent manner to detect lateral segregation in model membranes. In particular, it is demonstrated that the Porod invariant, $Q = \int q^2 I(q)\,\mathrm{d}q$, is related to the scattering length density contrast between compositionally distinct regions in a heterogeneous membrane. The formation of domains and the concomitant identification of phase boundaries as a function of either membrane composition or temperature can therefore be detected in the changes taking place in Q.

1. Introduction

Membranes form the interfaces that encompass and define cells, and biological tissue (Alberts *et al.*, 1989). Thus, a cell membrane forms a barrier that contains the components that make up a cell, and also acts as the site of contact for cell recognition and communication. Although cell membranes are composed of both lipids and proteins, the lipid components can self-assemble in water to form pure lipid membranes that share many properties with their cellular counterparts. Lipid membranes have thus found extensive use as model systems for biochemical studies and as biocompatible interfaces in technological development.

Although the concept is by no means new (see *e.g.* Edidin, 2001, and references therein), the notion that lateral organization of cell membranes may play a role in biological function has recently stimulated a flurry of both experimental (*e.g.* Silvius, 2003; Veatch *et al.*, 2004; Kahya *et al.*, 2005; Hammond *et al.*, 2005; Orädd *et al.*, 2005; Pencer *et al.*, 2005; Masui *et al.*, 2006) and theoretical studies (*e.g.* Kumar *et al.*, 2001; Lipowsky & Dimova, 2003; Yamamoto & Hyodo, 2003; Pandit *et al.*, 2004; Zuckermann *et al.*, 2004) examining lateral organization and heterogeneity in a variety of model membrane systems. Of the many techniques employed, fluorescence microscopy has been very popular, while small-angle scattering (SAS) has found the least use in characterizing laterally heterogeneous model membranes. We suspect that the popularity of visually based techniques over scattering is a consequence of the relative complexity in the analysis and interpretation of scattering data. Nevertheless, despite the disadvantages of complex analysis, SAS has a distinct advantage over microscopic techniques in that it is capable of probing nanometre length scales and yielding ensemble-averaged information.

In a previous study, we have demonstrated that, through the appropriate use of selective deuteration, it is possible to use small-angle neutron scattering (SANS) to characterize lateral heterogeneities in model membrane systems (Pencer *et al.*, 2005). In order to make the SAS technique more amenable for use in studies of laterally heterogeneous membranes, we devise here a quantitative model-independent method for detecting lateral segregation in model membranes by SAS.

2. The scattering function, $I(q)$

The variation of scattered intensity as a function of q from a vesicle with arbitrary scattering length density (SLD) can be determined by the equation (Moody, 1975)

$$I(q) = n\frac{1}{q^2}\left[\int_{\mathbf{r}} g(\mathbf{r})\exp(\mathbf{q}\cdot\mathbf{r})\,\mathrm{d}\mathbf{r}\right]^2, \qquad (1)$$

or, alternatively *via* the Debye expression (Feigin & Sholer, 1975)

$$I(q) = n\int\int g(\mathbf{r})g(\mathbf{r}')\frac{\sin q|\mathbf{r}-\mathbf{r}'|}{q|\mathbf{r}-\mathbf{r}'|}\,\mathrm{d}\mathbf{r}\,\mathrm{d}\mathbf{r}', \qquad (2)$$

where the origin lies at the centre of the vesicle. $g(\mathbf{r}) = \rho(\mathbf{r}) - \rho_s$ is the SLD contrast, $\rho(\mathbf{r})$ is the (neutron or X-ray) SLD of the object, which may vary within the volume of the object, n is the number density of vesicles in solution, and ρ_s is the mean SLD of the medium or solvent. In the following discussion, the scattered intensity, $I(q)$, will be normalized with respect to the number density n.

In the case of vesicles with nonuniform SLD, the SLD, $\rho(\mathbf{r})$, can be represented as a sum of two contributions: an orientationally averaged contribution $\rho_{0,0}(r)$, given by

$$\rho_{0,0}(r) = \frac{1}{4\pi}\int_0^{\pi}\sin\theta\int_0^{2\pi}\rho(r,\theta,\varphi)\,\mathrm{d}\varphi\,\mathrm{d}\theta, \tag{3}$$

where r, θ and φ are the spherical coordinates of a mass element within the vesicle membrane. The origin is again located at the centre of the vesicle. An orientationally fluctuating component, $\rho_{\rm f}(r,\theta,\varphi)$, is then given by

$$\rho_{\rm f}(r,\theta,\varphi) = \rho(r,\theta,\varphi) - \rho_{0,0}(r). \tag{4}$$

We can further define a radially averaged SLD, $\bar{\rho}$, as

$$\bar{\rho} = \frac{4\pi}{V}\int_0^{\infty} r^2\rho_{0,0}(r)\,\mathrm{d}r, \tag{5}$$

and a fluctuating radial SLD component, $\rho_{\rm r}(r)$:

$$\rho_{\rm r}(r) = \rho_{0,0}(r) - \bar{\rho}. \tag{6}$$

Thus, the membrane SLD can be expressed as a sum of three contributions:

$$\rho(r,\theta,\varphi) = \bar{\rho} + \rho_{\rm r}(r) + \rho_{\rm f}(r,\theta,\varphi), \tag{7}$$

where $\bar{\rho}$ is the mean SLD, $\rho_{\rm r}(r)$ is a radially fluctuating component of the SLD that does not vary with θ or φ, and $\rho_{\rm f}(r,\theta,\varphi)$ is the fluctuating component of the SLD that describes the lateral heterogeneity of the membrane.

We have shown previously (Pencer *et al.*, 2005) that the scattered intensity from laterally heterogeneous vesicles can be described as a sum of three contributions: (i) $F_{\rm ave}(q)$, the scattered amplitude due to the mean SLD (averaged both radially and orientationally), (ii) the amplitude due to the radially fluctuating orientationally averaged SLD, $F_{\rm r}(q)$, and (iii) the laterally heterogeneous contribution of ρ, given by $F_{\rm f}(q)$. The sum of these three contributions gives the total scattered intensity

$$I(q) = [F_{\rm ave}(q) + F_{\rm r}(q) + F_{\rm f}(q)]^2. \tag{8}$$

Under contrast matching conditions, $\rho_{\rm s} = \bar{\rho}$, and $F_{\rm ave}(q) = 0$, resulting in

$$I_{\rm match}(q) = [F_{\rm r}(q) + F_{\rm f}(q)]^2. \tag{9}$$

While studies elsewhere have provided straightforward analytic forms for the radially fluctuating SLD contribution to the scattering curve, $F_{\rm r}(q)$ (see *e.g.* Kučerka *et al.*, 2004; Pencer *et al.*, 2006), the laterally fluctuating SLD contribution, $F_{\rm f}(q)$, depends in a complex way on the size, number and shape of domains present on a vesicle. As such, without additional information (*i.e.* the total area or composition of domains) fitting $I(q)$ to a model scattering curve is non-trivial (Pencer *et al.*, 2005).

3. The scattering invariant, Q

While the determination of parameters such as domain size, number and shape depends on specific vesicular form factor models, it is possible to detect domains or lateral heterogeneities without having to rely on such models. The mean square fluctuation in the SLD, which is related to both radial and lateral membrane heterogeneities, is an invariant quantity that can be related to the integral of the scattered intensity in reciprocal space (*e.g.* Porod, 1951, 1982). This invariant, sometimes called the Porod invariant, Q, is given as (Hickl & Ballauff, 1997)

$$Q = \int I(q)q^2\,\mathrm{d}q = 2\pi^2\int g^2(\mathbf{r})\,\mathrm{d}\mathbf{r}. \tag{10}$$

Substitution of equation (7) into equation (10) gives

$$\begin{aligned} Q = 2\pi^2\int r^2\,\mathrm{d}r\int\sin\theta\,\mathrm{d}\theta\int\mathrm{d}\varphi\Big\{&(\bar{\rho}-\rho_{\rm s})^2 \\ &+ 2(\bar{\rho}-\rho_{\rm s})\big[\rho_{\rm r}(r)+\rho_{\rm f}(r,\theta,\varphi)\big] \\ &+ \big[\rho_{\rm r}(r)+\rho_{\rm f}(r,\theta,\varphi)\big]^2\Big\}. \end{aligned} \tag{11}$$

From the definitions of $\rho_{\rm r}(r)$ and $\rho_{\rm r}(r,\theta,\varphi)$, equation (11) simplifies to

$$\begin{aligned} Q = 2\pi^2\int r^2\,\mathrm{d}r\int\sin\theta\,\mathrm{d}\theta\int\mathrm{d}\varphi\Big\{&(\bar{\rho}-\rho_{\rm s})^2 \\ &+ \big[\rho_{\rm r}(r)\big]^2+\big[\rho_{\rm f}(r,\theta,\varphi)\big]^2\Big\}. \end{aligned} \tag{12}$$

Thus, the calculation of Q yields a sum of three terms, Q_0, $Q_{\rm r}$ and $Q_{\rm f}$, which are related, respectively, to the square of the mean SLD contrast, the mean square radial fluctuation in SLD, and the mean square lateral fluctuation in SLD. The three invariant components are given by

$$\begin{aligned} Q_0 &= 2\pi^2V(\bar{\rho}-\rho_{\rm s})^2, \\ Q_{\rm r} &= 2\pi^2\int 4\pi r^2\,\mathrm{d}r\big[\rho_{\rm r}(r)\big]^2, \\ Q_{\rm f} &= 2\pi^2\int r^2\,\mathrm{d}r\int\sin\theta\,\mathrm{d}\theta\int\mathrm{d}\varphi\big[\rho_{\rm f}(r,\theta,\varphi)\big]^2, \end{aligned} \tag{13}$$

where V is the volume of the vesicle membrane.

Note that the zero-angle scattered intensity $I(0)$ is related to Q_0 by

$$Q_0 = 2\pi^2I(0)/V. \tag{14}$$

If the vesicle membrane volume is known then the combined contributions, $Q_{\rm r} + Q_{\rm f}$, from radial and lateral SLD fluctuations to the invariant, Q, can be calculated from

$$Q_{\rm r} + Q_{\rm f} = Q - 2\pi^2I(0)/V, \tag{15}$$

where the invariant Q and forward scattered intensity $I(0)$ can be evaluated from the experimentally determined scattering curve. If measurements are performed at contrast matching conditions, $\bar{\rho} = \rho_{\rm s}$, $I(0) = 0$, and $Q = Q_{\rm r} + Q_{\rm f}$.

4. Determination of lateral fluctuations, $Q_{\rm f}$

While extracting the contribution $Q_{\rm r} + Q_{\rm f}$ from the total invariant Q may seem straightforward, the separation of $Q_{\rm f}$ and $Q_{\rm r}$ is not as simple and requires some knowledge of the structure and chemical composition of the membrane.

A unilamellar vesicle (ULV) is a hollow shell, containing and surrounded by an aqueous medium, and composed of a lipid bilayer. The lipids making up the bilayer have hydrophilic headgroups and hydrophobic acyl chains and arrange themselves so that the hydrophilic headgroups are oriented toward the membrane–water interface. Because they have different chemical compositions, the lipid headgroups and acyl chains also differ from each other in their SLD, and contrast with the aqueous medium. Thus Q_r appears to arise from two contrast terms, $(\rho_{ac} - \bar{\rho})$, the contrast between the (mean) lipid acyl chain SLD and the mean lipid SLD, and $(\rho_h - \bar{\rho})$ the contrast between the (mean) lipid headgroup SLD and the mean lipid SLD. However, substitution of $\bar{\rho}$ with $\bar{\rho} = (V_{ac}\rho_{ac} + V_h\rho_h)/V$ reveals that Q_r arises from the contrast term, $(\rho_{ac} - \rho_h)$. Consequently,

$$\begin{aligned} Q_r &= 2\pi^2\left[V_{ac}(\rho_{ac} - \bar{\rho})^2 + V_h(\rho_h - \bar{\rho})^2\right] \\ &= 2\pi^2 \frac{V_{ac}V_h}{V}(\rho_{ac} - \rho_h)^2, \end{aligned} \tag{16}$$

where V_{ac} and V_h are the total volumes and ρ_{ac} and ρ_h are the laterally averaged SLDs of the acyl chain and lipid headgroup regions, respectively. The invariant quantity, Q_f, that describes the scattering from ULV membrane lateral heterogeneities can then be calculated from

$$\begin{aligned} Q_f &= Q - \frac{2\pi^2}{V}\left[I(0) + V_{ac}V_h(\rho_{ac} - \rho_h)^2\right] \\ &= Q - \frac{2\pi^2}{V}\left[V^2(\bar{\rho} - \rho_s)^2 + V_{ac}V_h(\rho_{ac} - \rho_h)^2\right]. \end{aligned} \tag{17}$$

The calculation of Q_f from a measured SAS curve can then be performed, given knowledge of the total membrane volume, V, and the volumes, V_{ac} and V_h, and mean SLD, $\bar{\rho}$, ρ_{ac} and ρ_h, of the membrane, acyl chain and headgroup regions, respectively. Alternatively, independent measurements of Q_r and Q_0 can be made.

5. SLD and area fraction of membrane domains

It now remains to show the relationship between the lateral fluctuation invariant Q_f and the SLD and area fraction of membrane lateral heterogeneities or domains. For simplicity, we will assume: (i) that the membrane surface is separated into domains of two types, 1 and 2, and (ii) that the interfaces between regions of 1 and 2 are sharp. Q_f is then given by

$$\begin{aligned} Q_f = {} & V_{1,ac}(\rho_{1,ac} - \bar{\rho}_{ac})^2 + V_{1,h}(\rho_{1,h} - \bar{\rho}_h)^2 \\ & + V_{2,ac}(\rho_{2,ac} - \bar{\rho}_{ac})^2 + V_{2,h}(\rho_{2,h} - \bar{\rho}_h)^2, \end{aligned} \tag{18}$$

where $V_{i,ac}$ and $V_{i,h}$ are the total volumes of the acyl chain region and headgroup region, respectively, of domains of type i, $\rho_{i,ac}$ and $\rho_{i,h}$ are the SLDs of the acyl chain and headgroup regions, respectively, of domains of type i, and $\bar{\rho}_{ac}$ and $\bar{\rho}_h$ are the laterally averaged SLDs of the acyl chain and headgroup regions, respectively.

We define the area fractions of regions 1 and 2 by $a_1 = A_1/A$ and $a_2 = A_2/A$, where A is the total membrane surface area. We further define the thicknesses of regions 1 and 2 to be t_1 and t_2, respectively. The thicknesses of the headgroup and acyl chain regions of domains of type i are then $t_{i,h}$ and $t_{i,ac}$, respectively. The lateral fluctuation term, Q_f, is then related to the area fractions of regions 1 and 2, a_1 and a_2, respectively, by

$$\begin{aligned} Q_f = A\Big\{ & a_1\left[t_{1,ac}(\rho_{1,ac} - \bar{\rho}_{ac})^2 + t_{1,h}(\rho_{1,h} - \bar{\rho}_h)^2\right] \\ & + a_2\left[t_{2,ac}(\rho_{2,ac} - \bar{\rho}_{ac})^2 + t_{2,h}(\rho_{2,h} - \bar{\rho}_h)^2\right]\Big\}. \end{aligned} \tag{19}$$

We can further simplify Q_f if we assume that the lipid headgroup SLD and thickness are the same in regions 1 and 2. Such an assumption is reasonable for mixtures where the lipid components have the same headgroup moieties, *e.g.* mixtures of unsaturated and saturated phosphatidylcholines:

$$Q_f \simeq A\left[a_1 t_{1,ac}(\rho_{1,ac} - \bar{\rho}_{ac})^2 + (1 - a_1)t_{2,ac}(\rho_{2,ac} - \bar{\rho}_{ac})^2\right]. \tag{20}$$

Rearrangement of equation (20) gives Q_f as a function of the area fraction of region 1, a_1, and SLD contrast between domains, $(\rho_1 - \rho_2)$:

$$\frac{Q_f}{A} = a_1(1 - a_1)(\rho_{1,ac} - \rho_{2,ac})^2 \frac{t_{1,ac}t_{2,ac}}{a_1 t_{1,ac} + (1 - a_1)t_{2,ac}}. \tag{21}$$

Clearly, Q_f can have non-zero values only when domains are formed. If we assume that the difference in acyl chain lengths in different regions of the heterogeneous membrane is small, *i.e.* $t_{1,ac} \simeq t_{2,ac}$, then

$$\frac{Q_f}{A t_{ac}} \simeq a_1(1 - a_1)\left(\rho_{1,ac} - \rho_{2,ac}\right)^2 \tag{22}$$

Thus, Q_f depends on two parameters, a contrast term, $(\rho_{1,ac} - \rho_{2,ac})$, corresponding to the SLD difference between compositionally distinct regions 1 and 2, and the area fraction a_1 of region 1 (or equivalently that of region 2, $a_2 = 1 - a_1$). Equations (21) and (22) both show that Q_f is proportional to $(\rho_{1,ac} - \rho_{2,ac})^2$, and a_1. For laterally homogeneous membranes, $Q_f = 0$, while heterogeneous vesicles show $Q_f \neq 0$. Therefore, an increase in Q_f from zero clearly indicates the formation of domains. Most likely, discontinuous or rapid changes in non-zero values of Q_f as a function of either membrane composition or temperature also indicate phase boundaries. Consequently, the measurement of changes in Q_f as a function of either membrane composition or temperature can therefore be used to detect both the onset of lateral segregation and corresponding phase boundaries in both composition and temperature. Note, however, that while Q_f can be used to detect domains, it is not possible to use Q_f to determine independently the domain size and composition, as shown in Appendix *A*.

6. Predictions for a two-component mixture

Below, we calculate the invariant Q and its components for a lipid mixture whose phase diagram is known. The calculations and plots that follow will aid in formulating the optimal experimental conditions for detecting domain formation.

Table 1
Relative fraction of deuterated DPPC (c), mean SLD ($\bar{\rho}$), mean acyl chain SLD (ρ_{ac}) and mean headgroup SLD (ρ_h) for a 1:1 mixture of DLPC:DPPC at 293 K.

The molar ratio of DPPC to DLPC in the liquid phase is 0.24:0.76, while that in the solid phase is 0.82:0.18. The liquid phase occupies a relative area $a_1 = 0.55$.

c	$\bar{\rho}$ (fm Å^{-3})	ρ_{ac}	ρ_h	$\rho_{ac,1}$	$\rho_{ac,2}$
0	0.027	−0.037	0.176	−0.038	−0.037
0.5	0.171	0.169	0.176	0.069	0.274
1.0	0.315	0.376	0.176	0.176	0.585

The phase diagram for mixtures of DPPC with DLPC has been well studied by techniques such as differential scanning calorimetry (see *e.g.* van Dijck *et al.* 1977). Over the temperature range from ∼273 to ∼303 K, this mixture shows lateral segregation into a solid phase, rich in DPPC, and a liquid phase, rich in DLPC. The phase diagram gives both the compositions and area fractions of the liquid and solid domains (regions 1 and 2, respectively), which we use to investigate the influence of lateral segregation and contrast conditions on the invariant Q, and its components Q_0, Q_r and Q_f. Table 1 gives the compositions and area fractions of regions 1 and 2 for several levels of DPPC deuteration, c. Note that, since $a_2 = 1 - a_1$, a_2 is not given in the table.

As can be seen above in equations (13), (16) and (22), there are three contrast terms which contribute to the invariant, Q: (i) the contrast between the mean membrane SLD and the medium, $(\bar{\rho} - \rho_s)$, (ii) the contrast between the mean SLD of the lipid headgroups and mean SLD of the acyl chain region, $(\rho_{ac} - \rho_h)$, and finally, (iii) the contrast between the acyl chain portions of regions 1 and 2, $(\rho_{ac,1} - \rho_{ac,2})$. The optimal conditions for the measurement of membrane lateral segregation therefore require contrast conditions which minimize (i) and (ii) while maximizing (iii).

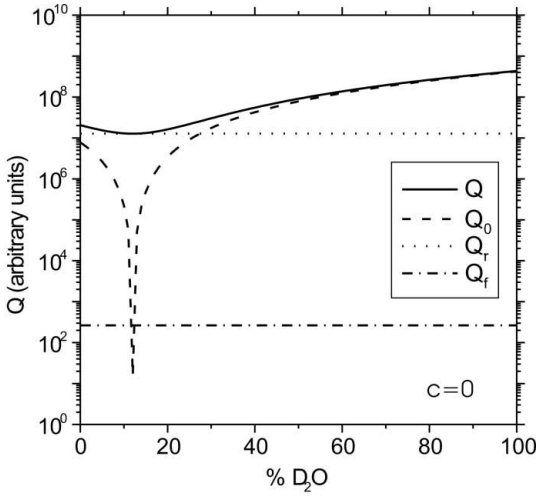

Figure 1
The invariant, Q (solid line), and its components, Q_0 (dashed line), Q_r (dotted line) and Q_f (dash-dotted line) plotted as a function of $\%D_2O$ content of the aqueous medium. Curves shown correspond to a 1:1 mixture of DPPC:DLPC at 293 K, with a deuterated DPPC relative fraction $c = 0$.

Figs. 1, 2 and 3 show plots of the invariant Q for 1:1 mixtures of DPPC:DLPC at 293 K, with 0, 0.5 and 1.0 relative fraction of deuterated DPPC, respectively, as a function of the $\%D_2O$ composition of the aqueous medium. In all three cases, we see that, at the contrast match point, where Q_0 is a minimum, Q results mainly from contributions from Q_r and Q_f. The relative fraction of deuterated DPPC, c, determines the relative contributions of Q_f and Q_r to Q. The parameter c also determines the extent of SLD contrast between regions 1 and 2, which has a minimum for no deuteration of DPPC (*i.e.* $c = 0$) and reaches a maximum value with maximum deuteration of DPPC, $c = 1.0$. The SLD contrast between the lipid headgroup and acyl chain region, on the other hand, is large when $c = 0$ and $c = 1$, and reaches a minimum at an intermediate value.

Table 1 shows that, when there is no deuterated DPPC in the DPPC:DLPC mixture, the SLD contrast between regions 1

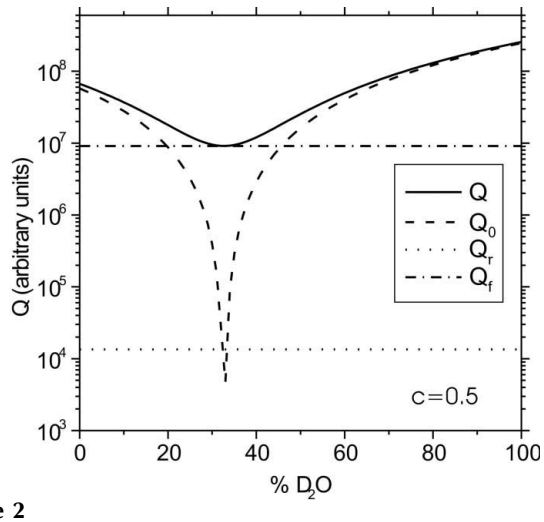

Figure 2
The invariant Q and its components are plotted similarly to Fig. 1. Curves are plotted for a 1:1 mixture of DPPC:DLPC at 293 K, with the relative fraction of deuterated DPPC, $c = 0.5$.

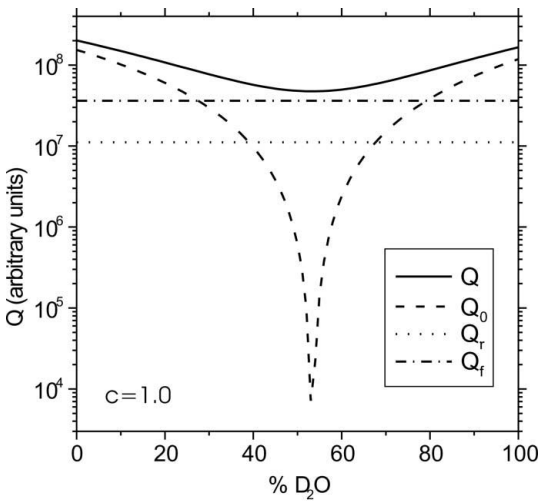

Figure 3
The invariant Q and its components are plotted similarly to Fig. 1. Curves are plotted for a 1:1 mixture of DPPC:DLPC at 293 K, with the relative fraction of deuterated DPPC, $c = 1.0$.

and 2 is small when compared with that between the mean acyl chain region and the headgroup region. This is illustrated quite dramatically in Fig. 1, which shows that the contribution of Q_r to Q is nearly five orders of magnitude higher than that from Q_f. Near the contrast match point, the value of Q essentially equals Q_r, while away from the match point, Q_0 becomes large compared with Q_r, dominating Q.

Increasing the fraction of chain perdeuterated DPPC in the lipid mixture increases the magnitude of Q_f, with respect to both Q_0 and Q_r. For $c = 0.5$, Table 1 shows that the mean acyl chain SLD has a value close to that of the lipid headgroups. Consequently, Q_r is small compared with Q_f. As seen in Fig. 2, the value of Q near the contrast match point is very close to Q_f, while, again, away from the match point, Q_0 becomes large compared with Q_r and Q_f and dominates the invariant Q.

For the maximum level of deuteration of DPPC, $c = 1.0$, Q_f reaches its maximum value. However, both Table 1 and Fig. 3 show that the SLD contrast between the lipid headgroup and acyl chain region also increases, with a concomitant increase in Q_r, compared with their values at $c = 0.5$. Fig. 3 shows that both Q_r and Q_f make a significant contribution to Q, at the contrast match point. As in the previous two cases, away from the match point, Q_0 becomes large compared with Q_r and Q_f and dominates the invariant Q.

Consequently, while, on the one hand, complete deuteration of one of the lipid components will give a maximum in the signal Q_f, there is also a large signal from Q_r. Unless Q_r can be accurately measured, independent of Q_f, the optimal conditions for the determination of Q_f correspond to contrast matching of the mean lipid SLD, *i.e.* $\bar{\rho} = \rho_s$, and small contrast between mean lipid acyl chain region and headgroups, *i.e.* $\rho_h \simeq \rho_{ac}$.

7. The problem of finite *q*

In practice, it is not possible to determine accurately the scattered intensity at high q, because of the rapid decrease in intensity with increasing scattering vector. The determination of the scattered intensity at low q is also difficult, although, in this case, because of the finite instrumental resolution. Consequently, the evaluation of the invariant Q is subject to errors due to the finite range of the scattering vector, q.

The problem of the accurate determination of Q has been discussed in detail by Kayushina *et al.* (1975), and more recently by Melnichenko *et al.* (2006). Evaluation of Q can be performed by numerical integration of the measured scattering curve plus estimations of the missing portions of the curve at low and high q. The low q contribution can be estimated *via* the Guinier approximation, $I(q) \simeq \exp -q^2 \mathrm{Rg}^2/3$, extrapolated from the measured intensity at the low q range, while the high q contribution can be estimated *via* the Porod approximation, $I(q) \simeq q^{-4}$. Melnichenko *et al.* (2006) estimate that the contribution to Q from data in the Guinier range is $\sim$1% of the total, while both Kayushina *et al.* (1975) and Melnichenko *et al.* (2006) estimate that data in the high-q Porod range can contribute as much as $\sim$20% of the total invariant. Thus, accurate determination of the invariant Q requires extrapolation of the scattered intensity at high q using the asymptotic behaviour of the scattering function. Nevertheless, when the contrast conditions are such that $Q = Q_f$, the partial evaluation of Q_f over finite q can still be used for the detection of domains, provided that q spans at least part of the range corresponding to the length scale characteristic of heterogeneities present.

8. Conclusions

In this paper, we outline a method for the detection of lateral heterogeneities in ULV by SAS. In particular, the technique lends itself to SANS, because of the unique sensitivity of SANS to contrast variation, *i.e.* H–D substitution. Nevertheless, SAXS could also be employed, where, *e.g.* sucrose addition and lipid bromination could be used as strategies for contrast variation of the medium and membrane, respectively. Unfortunately, while the invariant Q can be used effectively as an indicator for lateral segregation, Q alone cannot be used to determine parameters such as domain area fraction or molecular composition.

Consequently, the determination of parameters such as domain area fraction and composition relies on fitting experimental data with the appropriate form factor. Motivated by the present results, we are now developing a general method for the calculation of form factors for heterogeneous vesicles. Our derivation of an analytic form factor for ULV with a single circular domain demonstrates that fits to experimental data can be used to determine both the domain size and composition in heterogeneous two-component vesicles. These results will be presented in part II of this series of articles.

APPENDIX *A*
Domain composition: the special case of two-component mixtures

The discussion below follows from the assumptions and final result of §5. If only two lipid components, types 'a' and 'b', are present in the mixed lipid vesicle, then the acyl chain SLDs of regions 1 and 2, $\rho_{1,ac}$ and $\rho_{2,ac}$, are

$$\rho_{1,ac} = \frac{n_{a,1} V_a \rho_a + n_{b,1} V_b \rho_b}{V_1}, \tag{23}$$

$$\rho_{2,ac} = \frac{n_{a,2} V_a \rho_a + n_{b,2} V_b \rho_b}{V_2}, \tag{24}$$

where V_i is the acyl chain volume of region i, $n_{x,i}$ is the number of lipids of type x in region i, V_x is the volume and ρ_x the SLD of lipid acyl chains of type x.

Given our assumption that the thicknesses of regions 1 and 2 are approximately equal, we can replace V_x and V_i by a_x and a_i, where a denotes the relative area fraction. We then obtain

$$\rho_{1,ac} = \frac{n_{a,1} a_a \rho_a + n_{b,1} a_b \rho_b}{a_1}, \tag{25}$$

$$\rho_{2,\mathrm{ac}} = \frac{n_{\mathrm{a},2}a_{\mathrm{a}}\rho_{\mathrm{a}} + n_{\mathrm{b},2}a_b\rho_{\mathrm{b}}}{a_2}. \quad (26)$$

Suppose that some relative fraction, c of component 'a' is deuterated, with acyl chain SLD ρ_{da}. The acyl chain SLDs of regions 1 and 2 can then be expressed as

$$\rho_{1,\mathrm{ac}} = \frac{(1-c)n_{\mathrm{a},1}a_{\mathrm{a}}\rho_{\mathrm{a}} + n_{\mathrm{b},1}a_{\mathrm{b}}\rho_{\mathrm{b}}}{a_1} + \frac{cn_{\mathrm{a},1}a_{\mathrm{a}}\rho_{\mathrm{da}}}{a_1}, \quad (27)$$

$$\rho_{2,\mathrm{ac}} = \frac{(1-c)n_{\mathrm{a},2}a_{\mathrm{a}}\rho_{\mathrm{a}} + n_{\mathrm{b},2}a_{\mathrm{b}}\rho_{\mathrm{b}}}{a_2} + \frac{cn_{\mathrm{a},2}a_{\mathrm{a}}\rho_{\mathrm{da}}}{a_2}. \quad (28)$$

Recall, from equation (22), that the invariant Q_{f} is proportional to the difference $\rho_{1,\mathrm{ac}} - \rho_{2,\mathrm{ac}}$. Subtraction of equation (26) from equation (25) gives

$$\rho_{1,\mathrm{ac}} - \rho_{2,\mathrm{ac}} = \frac{a_{\mathrm{a}}\left(a_1 n_{\mathrm{a}} - n_{\mathrm{a},1}\right)}{a_1(a_1-1)}\left[(1-c)\rho_{\mathrm{a}} + c\rho_{\mathrm{da}} - \rho_{\mathrm{b}}\right], \quad (29)$$

where n_{a} is the total number of lipids per vesicle of type 'a'. Substitution of equation (27) into equation (22) then gives

$$\frac{Q_{\mathrm{f}}}{At_{\mathrm{ac}}} \simeq a_{\mathrm{a}}^2\left(n_{\mathrm{a},1} - a_1 n_{\mathrm{a}}\right)^2\left[(1-c)\rho_{\mathrm{a}} + c\rho_{\mathrm{da}} - \rho_{\mathrm{b}}\right]^2. \quad (30)$$

Typically, the parameters ρ_{a}, ρ_{b}, ρ_{da}, a_{a} and n_{a} are known or can be measured by complementary techniques. The parameter c, the relative fraction of component 'a' that is deuterated, is defined experimentally. This then leaves the parameters a_1, the relative area fraction of region 1, and $n_{\mathrm{a},1}$, the number of lipids of type 'a' in region 1, as unknowns. Unfortunately, our theoretical analysis shows that it is impossible to use Q_{f} alone to determine independently the relative area fraction or composition of domains, by varying the isotopic composition either of the solvent or the lipids.

The authors thank T. T. Mills, R. M. Epand, S. Krueger and M.-P. Nieh for valuable discussions and advice.

References

Alberts, B., Bray, D., Lewis, J., Raff, M., Roberts, K. & Watson, J. D. (1989). *Molecular Biology of the Cell*. New York: Garland Publishing.

Dijck, P. W. M. van, Kaper, A. J., Oonk, H. A. J. & de Gier, J. (1977). *Biochim. Biophys. Acta*, **470**, 58–69.

Edidin, M. (2001). *Trends Cell Biol.* **11**, 492–496.

Feigin, L. A. & Sholer, I. (1975). *Sov. Phys. Crystallogr.* **20**, 302–305.

Hammond, A. T., Heberle, F. A., Baumgarte, T., Holowka, D., Baird, B. & Feigenson, G. W. (2005). *Proc. Natl Acad. Sci.* **102**, 6320–6325.

Hickl, P. & Ballauff, M. (1997). *Physica A*, **235**, 238–247.

Kahya, N., Brown, D. A. & Schwille, P. (2005). *Biochemistry*, **44**, 7479–7489.

Kayushina, R. L., Rol'bin, Yu. A. & Feigin, L. A. (1975). *Sov. Phys. Crystallogr.* **19**, 722–724.

Kumar, P. B. S., Gompper, G. & Lipowsky, R. (2001). *Phys. Rev. Lett.* **86**, 3911–3914.

Kučerka, N., Nagle, J. F., Feller, S. E. & Balgavý, P. (2004). *Phys. Rev. E*, **69**, 051903(1–7).

Lipowsky, R. & Dimova, R. (2003). *J. Phys. Condens. Matter*, **15**, S31–S45.

Masui, T., Imai, M. & Urakami, N. (2006). *Physica B.* In the press.

Melnichenko, Y. B., Wignall, G. D., Cole, D. R. & Frielinghaus, H. (2006). *J. Chem. Phys.* **124**, 204711(1–11).

Moody, M. F. (1975). *Acta Cryst.* A**31**, 8–15.

Orädd, G., Westerman, P. W. & Lindblom, G. (2005). *Biophys. J.* **89**, 315–320.

Pandit, S. A., Jakobsson, E. & Scott, H. L. (2004). *Biophys. J.* **87**, 3312–3322.

Pencer, J., Mills, T., Anghel, V., Krueger, S., Epand, R. M. & Katsaras, J. (2005). *Eur. Phys. J. E*, **18**, 447–458.

Pencer, J., Krueger, S., Adams, C. & Katsaras, J. (2006). *J. Appl. Cryst.* **39**, 293–303.

Porod, G. (1951). *Kolloid Z.* **124**, 83–114.

Porod, G. (1982). *Small Angle X-ray Scattering*, edited by O. Glatter & O. Kratky, pp. 17–51. New York: Academic Press.

Silvius, J. R. (2003). *Biophys. J.* **85**, 1034–1045.

Veatch, S. L., Polozov, I. V., Gawrisch, K. & Keller, S. L. (2004). *Biophys. J.* **86**, 2910–2922.

Yamamoto, S. & Hyodo, S. J. (2003). *Chem. Phys.* **118**, 7937–7943.

Zuckermann, M. J., Ipsen, J. H., Miao, L., Mouritsen, O. G., Nielsen, M., Polson, J., Thewalt, J., Vattulainen, I. & Zhu, H. (2004). *Methods Enzymol.* **383**, 198–229.